JOURNAL OF Materials CHEMISTRY

Copper nanoparticles in zeolite Y

Andreas Seidel,[a] Joachim Loos†[b] and Bruno Boddenberg*[a]

[a]*Lehrstuhl für Physikalische Chemie II, Department of Chemistry, University of Dortmund, Otto-Hahn-Str. 6, D-44227 Dortmund, Germany. E-mail: bod@pcii.chemie.uni-dortmund.de*
[b]*Lehrstuhl für Werkstoffkunde, Department of Chemical Engineering, University of Dortmund, Emil-Figge-Str. 66, D-44227 Dortmund, Germany*

Received 8th April 1999, Accepted 28th June 1999

CuCl has been dispersed in the supercages of a Y-type zeolite by heating a mechanical salt/host mixture *in vacuo*. The occluded salt was subsequently reduced to copper metal in a hydrogen atmosphere. Virtually complete reduction of the salt is achieved at 460 °C. Under the same conditions, extraframework copper(II) ions, exchanged into zeolite NaY, are only partly reduced. The copper forms nanoaggregates of narrow size distribution inside the zeolite pore system; the average particle diameter is 5 nm. Our data suggest that these nanoparticles consist of several interconnected copper assemblies of supercage (diameter 1.2 nm) size. A small fraction of the salt remains at the outer surface of the zeolite crystallites in the inclusion step, and there produces larger copper metal particles upon reduction with H_2.

Introduction

Small transition metal particles are known for their catalytic activity in a variety of chemical reactions.[1–4] Zeolites and other microporous solids are often used as the support for metal dispersions.[3–6] These supports either act as catalytically inert materials providing matrices of well defined micropores in which metal nanoparticles can be stabilized, or contain additional, in most cases acidic, sites that are catalytically active as well. In the latter case, the dispersed metal and the zeolite form a bifunctional catalyst.

The conventional procedure for producing metal dispersions in zeolites is to introduce metal cations into the zeolite framework by ion-exchange and, in a second step, to treat the dehydrated, ion-exchanged material in a reductive atmosphere, most commonly CO or H_2.[3–6] The disadvantages of this preparation scheme are two-fold. First, in many cases, high temperatures have to be applied in the reduction step to obtain good reduction levels. This is because at lower temperatures only part of the cations in the dehydrated zeolites are accessible to the reducing agent. Second, the concentration and size of metal particles achievable with this preparation route is limited by the amount of cations in the zeolite, which for dealuminated materials can be very low. To overcome the first disadvantage, vapours of volatile metals such as zinc, cadmium or alkali metal elements have been suggested as an alternative gas phase medium with high reduction potential.[5–9] Because of their small diameter, the metal atoms in the vapour will have easy access even to those cations that are at positions in the zeolite framework not readily accessible to bulkier gas molecules such as CO. However, there is the danger that these vapours may be adsorbed in the zeolite pores and form alloys with the active metal component. Such alloys might exhibit a modified catalytic activity compared to the pure metal. The second disadvantage can be addressed by using so-called impregnation techniques.[5,6,10] In this case, transition metal salts are deposited in the pores of the zeolite crystals. As before, the salt is reduced to the metal in a second preparation step. In some special cases, it is also possible to adsorb and decompose uncharged carbonyl metal complexes in the zeolite pores.[4–6]

An interesting alternative to the wet-impregnation technique is to introduce the reducible salt into the zeolite pores by a solid-state reaction. It has been repeatedly shown that salts can be included in the pores of different types of zeolites by heating mechanical zeolite/salt mixtures at elevated temperatures *in vacuo*.[11–13] The present investigation addresses the inclusion of a copper salt in the supercages of a faujasite-type zeolite, and evaluates the reducibility of the included salt to copper metal.

Experimental

The starting material for the present investigation was zeolite NaY(Br) which was prepared from the commercial material NaY (LZ-Y52, Union Carbide; Si : Al = 2.4) and crystalline NaBr (Merck) according to a procedure described elsewhere.[12,13] In comparison to the parent NaY, this zeolite has virtually all of the small cubooctahedra (β-cages) filled with one NaBr unit, whereas the supercages are chemically unchanged.[12,13] This salt occlusion leads to a greater thermal stability of the aluminosilicate framework[10] and restricts any further incorporation of material to the large supercages.

Zeolite NaY(Br) was thoroughly mixed with crystalline CuCl (Merck) in an amount corresponding to 8 CuCl per (1/8) unit cell (uc), and subsequently heated for 24 h at 420 °C under high vacuum conditions. The material so obtained is designated NaY(Br)/CuCl. This zeolite was reduced in hydrogen gas ($p = 30$ kPa) at 300 °C, and subsequently at 460 and 600 °C. At each temperature, the zeolite was contacted with hydrogen for a total of 2.5 h, replacing the reductive atmosphere by fresh hydrogen every 0.5 h. During each step, the total pressure in the preparation cell increased slightly indicating that the reaction $CuCl + 1/2H_2 = Cu + HCl$ was taking place. The reduced samples are denoted by the reduction temperature T, *i.e.* NaY(Br)/CuCl(T/°C). They exhibit a pink colouration the intensity of which increases with T. By contrast, the starting zeolite NaY(Br) was white, and the unreduced material NaY(Br)/CuCl was faintly grey.

For comparison purposes, a copper(II)-exchanged zeolite, designated CuY, was prepared from NaY by repeated ion-exchange with a 0.1 mol dm^{-3} aqueous solution of $Cu(NO_3)_2$ at 80 °C and pH = 5.0–5.5. X-ray fluorescence (XRF) spectroscopy was used to measure the degree of copper for sodium exchange which was found to be 80 ± 10%. This zeolite was dehydrated *in vacuo* at 400 °C for 16 h, and subsequently reduced for 3 h with hydrogen at 460 °C. This sample is denoted CuY(460).

†Present address: Dutch Polymer Institute, Eindhoven University of Technology, P.O. Box 513, 5600 MB Eindhoven, The Netherlands.

Transmission electron microscopy (TEM) at 200 kV (CM 200, Philips) was used to obtain images from samples NaY(Br)/CuCl(600) and CuY(460). Crystallites of these materials were embedded in epoxy resin that was thinned down to *ca.* 50 nm by ion beam milling using a Dual Ion Mill (Model 600, Gatan).

Adsorption isotherms of nitrogen at −196 °C, and of xenon and carbon monoxide at 25 °C were measured volumetrically using all-steel equipment. In the case of zeolite CuY(460), CO adsorption was measured at 140 °C in order to achieve a reasonably low equilibration time (*ca.* 1 h).

^{27}Al MAS NMR spectra were obtained with a solid-state NMR spectrometer (Bruker MSL 400, Karlsruhe, Germany) operating at the resonance frequency $\omega/2\pi = 104.26$ MHz. The 4 mm ZrO_2 rotors containing completely rehydrated zeolites NaY(Br)/CuCl(600) and CuY(460), were spun at the magic angle at 8 kHz. The chemical shift scale is referenced to 3 M aqueous $Al(NO_3)_3$ solution.

X-Ray powder diffractograms (Siemens D500 diffractometer) were measured for completely rehydrated zeolites NaY(Br)/CuCl(600) and CuY(460) using Cu-Kα radiation.

Results

Fig. 1 shows the ambient temperature CO adsorption isotherms of zeolites NaY(Br), NaY(Br)/CuCl and NaY(Br)/CuCl(T/°C) for $T = 300$, 460 and 600 °C. At each pressure, the highest adsorption is observed for the unreduced zeolite loaded with CuCl, *i.e.* NaY(Br)/CuCl. Here, a steep initial increase up to *ca.* 30 CO uc^{-1} at 5 kPa is followed by a much flatter region that eventually reaches *ca.* 40 CO uc^{-1} at 40 kPa. Reduction leads to a dramatic decrease in the isotherm. At $T = 460$ °C, the steep initial increase has almost disappeared, and at $T = 600$ °C, it has completely disappeared, leaving a linear isotherm coincident with the isotherm of NaY(Br).

In addition, Fig. 1 shows the CO adsorption isotherm of zeolite CuY(460) at 140 °C. In contrast to the CuCl-containing zeolite, reduction at 460 °C of this ion-exchanged material still leads to a strongly curved isotherm shape with an initial steep increase reaching 10 CO uc^{-1} at *ca.* 5 kPa.

Fig. 2(a)–(c) show brightfield TEM micrographs of zeolites NaY(Br)/CuCl(600) [(a) and (b)] and CuY(460) (c). Besides some large metal aggregates, only seen for NaY(Br)/CuCl(600) [Fig. 2(a) and (b)], copper nanoparticles of size of 5 ± 2 nm with rather uniform spatial distribution prevail in both specimens.

Fig. 3(a) and (b) show XRD powder diffractograms of samples NaY(Br)/CuCl(600) and CuY(460), respectively. The dominant XRD lines at $2\theta = 43.4$ and 50.5° of the former zeolite, are at the same positions as the Cu(111) and (200)

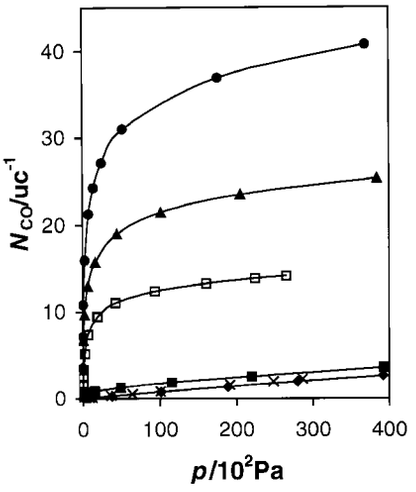

Fig. 1 CO adsorption isotherms of zeolites NaY(Br) (×), NaY(Br)/CuCl (●), NaY(Br)/CuCl(300) (▲), NaY(Br)/CuCl(460) (■), NaY(Br)/CuCl(600) (◆) and CuY(460) (□).

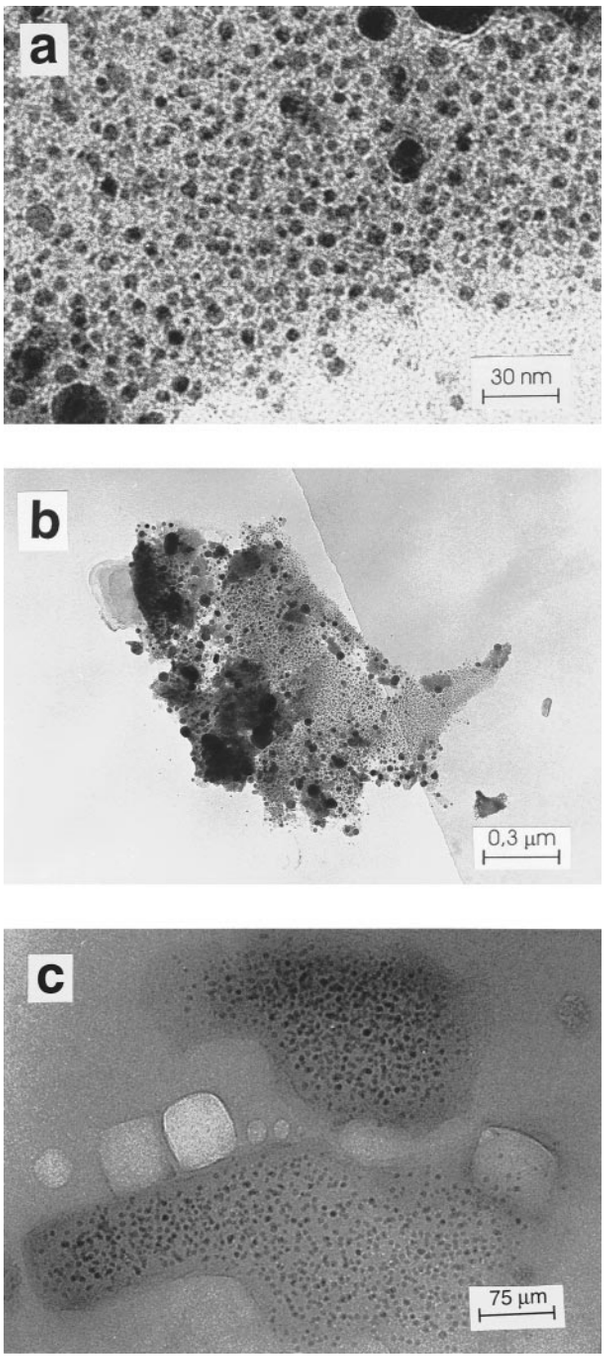

Fig. 2 Brightfield TEM pictures of zeolite NaY(Br)/CuCl(600) [(a) and (b)] and CuY(460) (c).

reflections, respectively, of bulk copper metal. The small width of these lines allows us to estimate a crystallite size of >30 nm suggesting that they originate from the larger copper particles seen in Fig. 2(a). The absence of bulk copper reflections in the diffractogram of sample CuY(460) [Fig. 3(b)] which shows no large agglomerates [Fig. 2(c)] confirms this interpretation. The diffraction angles of all the other lines are in quantitative agreement with literature data for zeolite NaY[14] indicating that the aluminosilicate framework has retained its crystallinity after the various preparation steps. This conclusion is confirmed by the absence of any signal at δ *ca.* 0 in the ^{27}Al MAS NMR spectra of both NaY(Br)/CuCl(600) and NaY(Br) (Fig. 4). Such signals would be indicative of octahedrally coordinated aluminium species resulting from framework destruction.[15] The only observed resonance line (at $\delta = 59$) is characteristic of the tetrahedrally coordinated aluminium atoms of the zeolite framework.[15]

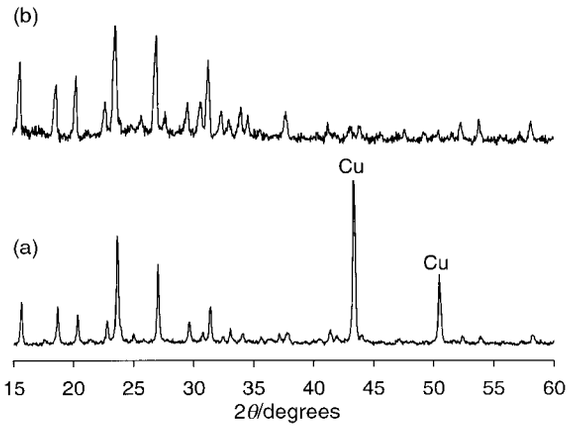

Fig. 3 X-Ray diffractograms of zeolite NaY(Br)/CuCl(600) (a) and CuY(460) (b).

Table 1 presents the specific pore volumes, V_p, of the zeolites NaY(Br), NaY(Br)/CuCl and NaY(Br)/CuCl(T/°C), each referred to the mass of dry zeolite NaY(Br). These data were calculated from the saturation capacities of the nitrogen adsorption isotherms at −196 °C (not shown) using Gurvitch's rule with $\rho^l(N_2) = 0.808$ g cm^{-3}.[16] The pore volume is highest for zeolite NaY(Br) and lowest for NaY(Br)/CuCl. The reduction of the latter sample with hydrogen leads V_p to increase with increasing reduction temperature. The value of V_p determined for NaY(Br)/CuCl(600) is lower by *ca.* 13% than the value for zeolite NaY(Br). Taking into account previous findings that zeolite NaY(Br) has virtually every β-cage filled with a NaBr unit,[13] the pore volume of this material, as referred to the mass of dry NaY, is calculated to be 0.33 cm^3 g^{-1}. This value is slightly lower than V_p reported for zeolite NaY (0.35 cm^3 g^{-1}).[12,14]

Fig. 5 shows the ambient temperature xenon adsorption isotherms of NaY(Br) and NaY(Br)/CuCl(600). In both cases, the isotherms are linear over the pressure range investigated. The slope of the isotherm of sample NaY(Br)/CuCl(600) is 9% lower relative to NaY(Br).

Discussion

It is well known that CO is very strongly bound by Cu^+ cations at accessible extraframework positions in zeolites[17–20]as well as by highly dispersed CuCl with formation of Cu(CO)Cl,[21–23] whereas on extraframework Cu^{2+} ions adsorption of CO is negligible at ambient temperature and above.[17,20] Adsorption of CO on copper metal (Cu^0) is generally considered to be weak although heats of adsorption in the range 46–64 kJ mol^{-1} for CO on copper dispersed on silica have been reported recently.[17]

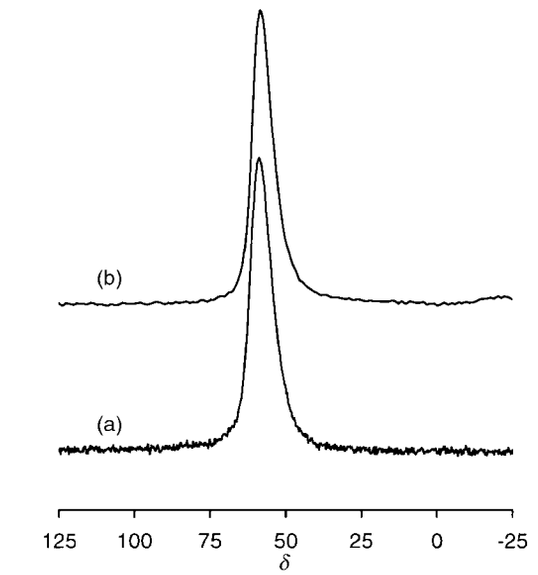

Fig. 4 ^{27}Al MAS NMR spectra of zeolite NaY(Br) before washing (a) and of NaY(Br)/CuCl(600) (b).

Table 1 Specific pore volumes determined from nitrogen saturation capacities

Sample	V_p/cm^3 g^{-1}	x_p[a]
NaY(Br)	0.31(1)	1.00
NaY(Br)/CuCl	0.14(1)	0.45
NaY(Br)/CuCl(300)	0.21(1)	0.68
NaY(Br)/CuCl(460)	0.27(1)	0.87
NaY(Br)/CuCl(600)	0.27(1)	0.87

[a] $x_P = V_p/V_p$[NaY(Br)].

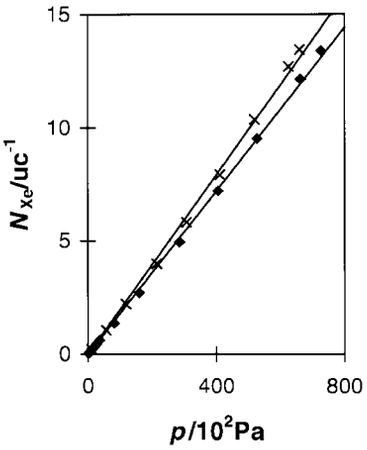

Fig. 5 Xe adsorption isotherms of zeolite NaY(Br) (×) and NaY(Br)/CuCl(600) (◆).

Based on this evidence, the very strong initial adsorption of CO in zeolite NaY(Br)/CuCl (Fig. 1) must be associated with dispersed CuCl. The lowering of this strong initial adsorption with increasing reduction temperature indicates consumption of CuCl which is complete at 600 °C. At 460 °C only a very small amount of CuCl appears to have remained unreduced. It is interesting that after reduction at 460 °C, zeolite CuY shows strong CO adsorption. In accordance with results from the literature,[24] this behaviour is ascribed to copper(I) ions generated by partial reduction of at least part of the copper(II) ions originally introduced by ion-exchange.

The adsorption isotherms of the reduced materials NaY(Br)-CuCl(T/°C) do not give any indication of CO adsorption on copper metal. This is clearly demonstrated for sample NaY(Br)CuCl(600) which shows the same linear CO adsorption isotherm as NaY(Br) within the range of experimental error. These findings, however, do not necessarily imply weak adsorption of CO at the dispersed copper nanoparticles inside the pores. It is also conceivable that the copper metal completely fills up part of the supercages available and leaves others unoccupied so that the adsorptive molecules are prevented from reaching metal surface sites. The larger particles as seen by TEM [Fig. 2(a) and (b)], however, exhibit a low surface to volume ratio such that adsorption of CO on these would contribute negligibly to the overall adsorption isotherm.

The copper nanoparticles of size 3–7 nm (TEM images, Fig. 2) are considerably larger than the supercages (diameter 1.2 nm). However, the observed even spatial distribution of these particles (Fig. 2) suggests that they reside inside the zeolitic pore system. Two explanations for the nature of these particles can be advanced. Either they consist of several

supercage-size clusters interconnected to each other within the crystalline aluminosilicate pore network, or they are compact particles generated in mesopores that result from a local destruction of the host.[25] The results of X-ray diffraction, where no line broadening is observed (Fig. 3), and of ^{27}Al NMR spectroscopy, where the resonance of tetrahedrally coordinated aluminium atoms remains the only detected signal (Fig. 4), are in favour of the first model. A similar 'cluster agglomerate' structure model has also been proposed for platinum and palladium metal particles in a faujasite type zeolite.[26] On the other hand, the absence (^{27}Al NMR) of non-tetrahedrally coordinated aluminium does not prove the absence of local framework destruction. It is conceivable that aluminium is contained in extraframework species at highly asymmetric sites or has been removed from the zeolite structure as a volatile chloride as a consequence of reaction with HCl produced by the reduction of CuCl with hydrogen. More detailed investigations are required in order to clarify this point.

The large copper particles in NaY(Br)/CuCl(600), which give rise to the copper XRD reflections [Fig. 3(a)] and can directly be seen by TEM [Fig. 2(a) and (b)], are considered to reside outside the zeolite crystallites and are believed to result from CuCl in the salt inclusion step that has remained at the outer surface. This indicates that the nominal amount of 8 CuCl per (1/8) uc used in the precursor mixture was too large to lead to complete dispersion in the cavities of the zeolite. This conclusion is at variance with the results of a previous study where a dispersion of 8.4 CuCl/supercage inside zeolite NaY was reported.[11] However, in that investigation a certain amount of CuCl may have also remained outside the zeolite crystals in dispersed, non-crystalline form, and so not have been detected by XRD.

The fraction of copper metal deposited inside the zeolite pore system can be assessed with the aid of the nitrogen adsorption data (Table 1). From the specific pore volume found for NaY(Br), the volume per supercage can be determined as $V_{sc}=8.85\times10^{-22}$ cm^3. We calculate that each of these supercages can shelter a cluster of *ca.* 75 Cu atoms, assuming the deposited copper particles to have the same density as the bulk metal ($\rho_{Cu}=8.94$ g cm^{-3}).[16] The nitrogen adsorption data in Table 1 show that the specific supercage volume of sample NaY(Br)/CuCl(600) is reduced by $13\pm6\%$ as compared to zeolite NaY(Br) and the reduction of the slope of the xenon adsorption isotherms by 9% observed for these samples falls into the same range. Ascribing this reduction of the nitrogen adsorption capacity to copper deposited inside the zeolite pores, we derive an average concentration of $13\pm6\%$ of 75, *i.e. ca.* 10 ± 4 Cu atoms deposited per supercage. Of course, this calculation has to be considered as an approximation that only provides an upper limit because the copper particles are not expected to fit snugly into the zeolite cavities, nor will the nanoparticles have exactly the same density as bulk copper. Nevertheless, comparison of the calculated concentration of deposited copper with the nominal amount of 8 CuCl per cage used in the salt occlusion step, suggests that the larger agglomerates at the outer surface of the microcrystallites constitute only a small fraction of the total copper in zeolite NaY(Br)/CuCl(600).

Conclusions

Considerable amounts of CuCl can be dispersed in the supercages of the aluminosilicate framework of zeolite NaY by a simple one-step solid-state procedure. The occluded CuCl can be completely reduced to copper metal nanoparticles under much milder conditions than are required for complete reduction of copper(II) cations at extraframework positions of such aluminosilicate materials. However, caution is necessary because some copper salt may remain at the outer surface of the zeolite crystallites, which may form larger copper metal particles upon reduction. By repetition of the salt inclusion/reduction cycle, the proposed preparation route will allow the attainment of much higher concentrations of metal particles in zeolite hosts than can be achieved with the conventional procedures applied so far.

Acknowledgement

Financial support by Deutsche Forschungsgemeinschaft (Schwerpunkt 'Nanoporöse Kristalle') is gratefully acknowledged.

References

1 *Metal Clusters in Catalysis*, ed. B. C. Gates, L. Guczi and H. Knözinger, *Stud. Surf. Sci. Catal.*, 1986, **29**.
2 *Metal-Support and Metal-Additive Effects in Catalysis*, ed. B. Imelik, C. Naccache, G. Coudurier, H. Praliaud, P. Meriaudeau, P. Gallezot, G. A. Martin and J. C. Vedrine, *Stud. Surf. Sci. Catal.*, 1982, **11**.
3 *Metal Microstructures in Zeolites: Preparation–Properties–Applications*, ed. P. A. Jacobs, N. I. Jaeger, P. Jiru and G. Schulz-Ekloff, *Stud. Surf. Sci. Catal.*, 1982, **12**.
4 D. Delafosse, *J. Chim. Phys. Phys.–Chim. Biol.*, 1986, **83**, 791.
5 P. A. Jacobs, *Stud. Surf. Sci. Catal.*, 1982, **12**, 71.
6 P. A. Jacobs, *Stud. Surf. Sci. Catal.*, 1986, **29**, 357.
7 K. Seff, *Stud. Surf. Sci. Catal.*, 1996, **102**, 267.
8 A. Seidel, F. Rittner and B. Boddenberg, *J. Phys. Chem. B*, 1998, **102**, 7176.
9 T. Sprang, A. Seidel, M. Wark, F. Rittner and B. Boddenberg, *J. Mater. Chem.*, 1997, **7**, 1429.
10 J. A. Rabo, in *Zeolite Chemistry and Catalysis*, ed. J. A. Rabo, *ACS Monograph 171*, American Chemical Society, Washington, DC, 1976, p. 332.
11 Y. Xie and Y. Tang, *Adv. Catal.*, 1990, **37**, 1.
12 A. Seidel, U. Tracht and B. Boddenberg, *J. Phys. Chem.*, 1996, **100**, 15917.
13 A. Seidel, B. Schimiczek, U. Tracht and B. Boddenberg, *Solid State NMR*, 1998, **12**, 53.
14 D. W. Breck, *Zeolite Molcular Sieves*, Robert E. Krieger, Malabar, 1984.
15 G. Engelhardt and D. Michel, *High-Resolution Solid-State NMR of Silicates and Zeolites*, John Wiley & Sons, Chichester, 1987.
16 *CRC Handbook of Chemistry and Physics*, ed. D. R. Lide, CRC Press, Boca Raton, FL, 78th edn., 1997.
17 G. D. Borgard, S. Molvik, P. Balaraman, T. W. Root and J. A. Dumesic, *Langmuir*, 1995, **11**, 2065.
18 J. Howard and J. M. Nicol, *Zeolites*, 1988, **8**, 142.
19 V. Borovkov and H. G. Karge, *J. Chem. Soc., Faraday Trans.*, 1995, **91**, 2035.
20 M. Hartmann and B. Boddenberg, *Microporous Mater.*, 1994, **2**, 127.
21 X. D. Peng, T. C. Golden, R. M. Pearlstein and R. Pierantozzi, *Langmuir*, 1995, **11**, 534.
22 W. Backen and R. Vestin, *Acta Chem. Scand., Ser A*, 1979, **33**, 85.
23 M. Håkansson and S. Jagner, *Inorg. Chem.*, 1990, **29**, 5241.
24 R. G. Herman, J. H. Lunsford, H. Beyer, P. A. Jacobs and J. B. Uytterhoeven, *J. Phys. Chem.*, 1975, **79**, 2388.
25 G. Schulz-Ekloff, in *Solid-State Supramolecular Chemistry: Two- and Three-Dimensional Inorganic Networks*, ed. G. Alberti and T. Bein, *Comprehensive Supramolecular Chemistry*, Pergamon, New York, 1996, vol. 7, p. 549.
26 G. Bergeret, P. Gallezot and B. Imelik, *J. Phys. Chem.*, 1981, **85**, 411.

Paper 9/02806D